View Online / Journal Homepage / Table of Contents for this issue
Dynamic Article Links

Journal of Materials Chemistry

Cite this: *J. Mater. Chem.*, 2011, **21**, 15464

www.rsc.org/materials

PAPER

Nanostructured LDH-container layer with active protection functionality

J. Tedim, M. L. Zheludkevich,* A. N. Salak, A. Lisenkov and M. G. S. Ferreira

Received 1st June 2011, Accepted 5th August 2011
DOI: 10.1039/c1jm12463c

Published on 05 September 2011 on http://pubs.rsc.org | doi:10.1039/C1JM12463C
Downloaded by Universidade de Aveiro (UAveiro) on 20 July 2012

Self-healing protective coatings based on different types of nanocontainers of corrosion inhibitors have been recently developed and reported as promising solutions for many industrial applications. Layered double hydroxide (LDH) nanocontainers are among the most interesting systems since they confer the delivery of inhibitors on demand under action of corrosion-relevant triggers such as the presence of corrosive anions or local change of pH. In this paper, we report for the first time a new approach based on formation of a nanostructured LDH-container layer directly on the metal surface as a result of conversion reaction with a metal (aluminium alloy 2024) surface. The methodology allows the formation of a spatially differentiated LDH structure preferentially on surface sites located at active intermetallics. The LDH container layer loaded with vanadate ions provides an efficient active corrosion protection and can be used as a functional layer in self-healing coating systems.

1. Introduction

The design of corrosion protective coatings for metallic materials is an issue of prime importance for a wide range of industrial applications including aeronautics, especially following the prohibition against the use of hexavalent chromium. Recently, a new concept based on *smart* nanocontainers for the enhancement of active anticorrosion performance in protective coatings has been considered as promising. Accordingly, nanocontainers are loaded with corrosion inhibitors and consequently dispersed in organic or hybrid coating matrices.[1–3] These nanomaterials have the ability to release inhibitors in a controlled manner, which can be tuned to coincide with an increase of the aggressiveness of the surrounding environment or corrosion initiation on the metallic substrates. In this way, the released inhibitors can suppress the corrosion reactions in the defected zones offering efficient self-healing ability to the protective coatings.

Layered Double Hydroxides (LDHs) loaded with corrosion inhibitor were recently reported as promising pigments to be used in self-healing protective coatings.[3,4] The release of anionic inhibitors from LDHs is triggered by the presence of corrosive chloride ions and proceeds according to anion-exchange reaction, thereby playing a double role: the release of inhibitors and entrapment of harmful chlorides. Buchheit and colleagues showed that the addition of Zn–Al LDH powders intercalated with decavanadate anions to organic resins led to improvement of corrosion protection of the aluminium alloy 2024 (AA2024).[3] Moreover, the structural changes observed when vanadate species are exchanged with chloride anions can be followed by XRD and be used as a method for indirect corrosion sensing. More recently, Buchheit *et al.* performed nuclear magnetic resonance measurements complemented by electrochemical studies in order to investigate the speciation of vanadates as a function of pH and vanadate concentration, and its effect on corrosion protection of AA2024 in NaCl solution.[5] It was found that the inhibition by vanadates mainly occurs in alkaline solutions where metavanadates and pyrovanadates are the most abundant. The corrosion inhibiting effect conferred by pyrovanadate ($V_2O_7^{2-}$) was also studied by Tedim and co-workers.[4] In this case, $V_2O_7^{2-}$ was intercalated with LDHs, and the resulting nanomaterials were found to render corrosion protection to AA2024 in NaCl solution.

The novel concept explored in this study is an extrapolation of the idea of *nanocontainer* to *nanostructured container layer* grown directly on the metallic substrate, using LDH crystallites as the 'building block' units (Scheme 1). One important advantage

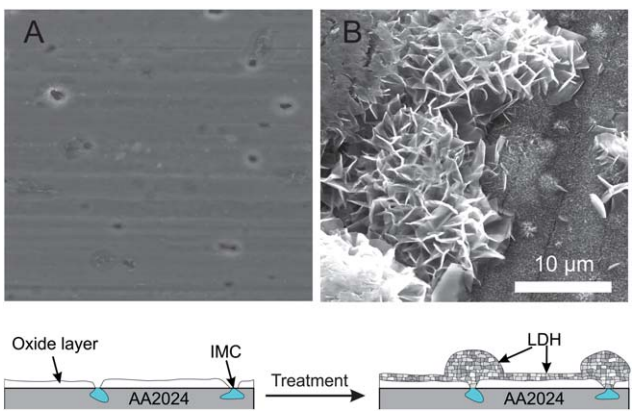

Scheme 1 SEM images of the bare substrate (A) and Zn–Al LDH intercalated with $V_2O_7^{2-}$ (B). Schematic presentation of selectively deposited LDH films.

CICECO, Dep. Ceramics and Glass Eng., University of Aveiro, 3810-193 Aveiro, Portugal. E-mail: mzheludkevich@ua.pt

This journal is © The Royal Society of Chemistry 2011

Published on 05 September 2011 on http://pubs.rsc.org | doi:10.1039/C1JM12463C
Downloaded by Universidade de Aveiro (UAveiro) on 20 July 2012

associated with direct growth on the surface when compared to applied coating layers is superior adhesion.[6–8] Moreover, there is a gain in terms of the inhibitor loading content and its proximity to the places where it is most needed: the metal surface. This functional layer can be regarded as a smart reservoir, meaning the ability to control the release of active species. The importance of such systems is transversal to many areas of science, due to the low-toxicity and biocompatibility of LDHs generally recognized by scientists.[9] From a corrosion-relevant perspective, such a functional layer can have a great impact on the global industry, mainly as an effective replacement for conventional pre-treatment layers on industrially relevant important metallic substrates.

Although there are several publications reporting on the formation of conversion films based on LDHs for Mg and Al alloys,[6–8,10–13] the methodologies are sometimes complex and do not rely on the differentiation of the surface. More specifically, they result in the formation of homogeneous films intercalated either with hydrophobic anions to confer hydrophobicity,[12,13] carbonate anions to decrease the exchangeability and to avoid the ingress of chlorides (passive barrier),[6,7,10,11] or even with oxidising agents that promote the sealing of pores.[14] Most of the routes mentioned above rely on the formation of LDHs *in situ*, but there are also studies involving the utilisation of pre-prepared LDH slurries[15] or application of pre-formed LDH powders by spin coating.[16]

In this paper, we present a very simple, yet elegant approach that can be used to grow spatially differentiated, nanostructured Zn–Al LDHs on the surface of aluminium alloys *in situ*. The applied methodology explores the weakness of the native aluminium oxide layer in the zones of intermetallic phases which are the most susceptible for localised corrosion attack. The source of aluminium cations necessary to grow the LDHs on the alloy surface is uneven, promoting differentiated growth of island-like LDHs on active intermetallics. The loading of corrosive inhibitor into the intergallery space of LDH by ion-exchange reaction creates nanostructured container islands on the active zones. With this approach, successful intercalation of corrosion inhibitor is achieved and the active corrosion protection is demonstrated for the first time.

2. Results and discussion

The LDH layers with nitrate anions were deposited on the aluminium alloy surface and later loaded with vanadate anions *via* an ion-exchange route, as described in the *Experimental* section. XRD patterns of the samples under study are depicted in Fig. 1. The diffraction pattern of a blank aluminium alloy 2024 plate treated with NaOH and HNO_3 is also presented for comparison purposes. In the samples with LDH-containing layers, well-resolved reflections typical of LDH phases are observed, along with the reflections intrinsic to the AA2024 alloy. Positions of the characteristic LDH reflections (003) and (006) of both as-prepared nitrate- and vanadate-containing samples (labeled as (2) and (3), respectively) were found to be in agreement with those previously observed in polycrystalline LDH powders with the same compositions, namely Zn(2)–Al–NO_3 and Zn(2)–Al–V_2O_7.[17] Moreover, no trace of the parent nitrate, LDH phase, has been revealed in the XRD pattern of the vanadate-containing sample. Thus, the anion-exchange reaction

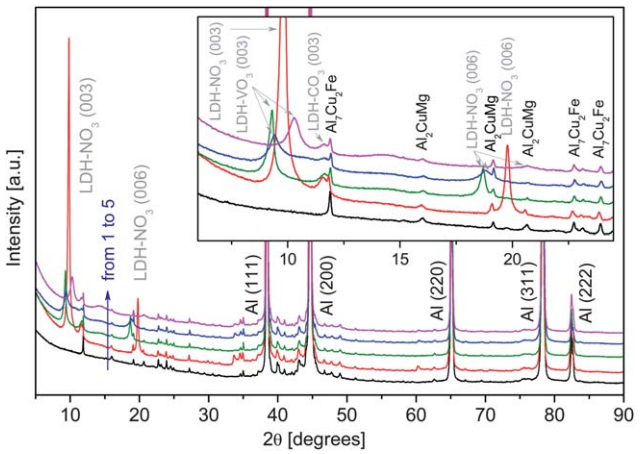

Fig. 1 XRD patterns of the AA2024 samples: blank surface (1), covered with Zn(2)Al–NO_3 (2), covered with Zn(2)Al–V_2O_7: as-prepared (3), immersed in 0.05 M NaCl for 2 weeks (4) and for 1 month (5). The inset shows the patterns at the ranges of (003) and (006) diffraction reflections. The reflections originated from the intermetallic inclusions in AA2024 are also indicated.

$NO_3^- \rightarrow V_2O_7^{2-}$ in the LDH layer was complete. This is the first time that an LDH layer with structurally intercalated corrosion inhibitors is obtained on the metal surface.

Additionally, a small diffraction peak was observed at ~11.5° (corresponding to a basal spacing of 0.765 nm), exhibiting similar intensity for all the LDH-containing samples (see the inset in Fig. 1). This peak was assigned to the (003) reflection of a phase of Zn(2)–Al–CO_3 composition.[18] This is due to the fact that the LDH synthesis was carried out under atmospheric conditions, leading to partial carbonation of the samples.[19] Although CO_3^{2-} is not a corrosion inhibitor *per se*, it can improve protective properties *via* formation of a very stable LDH structure. Permeation of such structures by anion-exchange (*e.g.* with corrosion-relevant anions) is unlikely to occur to a great extent. Besides, contamination with CO_2 can be avoided if additional precautions during the experimental procedure are taken, similar to those followed in the preparation of LDH powders.[3,4,20]

In a recent study, the nitrate-to-vanadate exchange in powder-like LDH nanocontainers has been shown to be accompanied by partial fragmentation of the crystallites.[17] If this process would occur in the case of the LDH layer studied in the present work, this structure would have become more porous after intercalation of $V_2O_7^{2-}$ as a result of fragmentation and the average crystallite size would decrease, being detectable by broadening of the diffraction lines. However, analysis of the XRD depicted in Fig. 1 shows that the broadening of diffraction peaks is not considerable in contrast to LDH-powders. This can be related to the different mechanism of fragmentation of LDH crystallites in both cases. LDH flakes formed on the alloy have less degrees of freedom since they are attached to the surface. In this case, only species from the outer parts of the 'islands', exposed to the vanadate-containing solution during the exchange process, break off from the layer. These small crystallites leave the LDH layer and do not contribute to its XRD pattern after anion exchange. Therefore, the average crystallite size remains nearly the same and no additional pores and defects appear in the layer.

Published on 05 September 2011 on http://pubs.rsc.org | doi:10.1039/C1JM12463C
Downloaded by Universidade de Aveiro (UAveiro) on 20 July 2012

The morphology and composition of the AA2024 surface after substrate preparation and LDH layer formation are also depicted in Scheme 1. After the substrate preparation (panel (A)), the AA2024 shows a flat surface with some holes corresponding to the removal of S-type intermetallic phases (IMC).[21] After the formation of LDH-vanadate, the morphology becomes completely different. The top view image depicted in panel (B) shows a differentiated surface, where micro-sized, nanostructured islands are dispersed and separated by a thin layer covering the rest of the surface. Proof of this covering layer is the different morphology when comparisons are made between the bare and LDH-container coated surfaces. The flake-like morphology typically found for LDH powders[22] is also observed in the case of the LDH deposited layer. The flakes are preferentially oriented perpendicular to the substrate, both in the islands and in the 'flat' areas. Such an oriented plate structure has been previously reported[8,13,14] and correlated with the faster crystal growth rate in the direction of bulk solution where the reactants are most accessible and the spatial restriction for growth is smaller. The cross-section of an LDH island is presented in detail in Fig. 2 (panel (A)) with the corresponding EDS analysis (panel (B)). Analysis of composition of the island reveals the presence of the main expected constituents: zinc, aluminium and vanadium, which supports the presence of LDHs intercalated with corrosion inhibitors. The thin LDH layer seems to be at least 4 times thinner (1–2 μm) than the LDH islands (8 μm). Furthermore, looking at the EDS map, the LDH island has been grown on top of a site where IMC phases existed (Cu is detected). It is known that the naturally occurring aluminium oxide film in aluminium alloys breaks down in the vicinity of IMC particles.[23] Consequently, the surface distribution of these LDH architectures reflects the availability of Al-soluble species. The dissolution rate of aluminium in the places of Cu-containing intermetallics is known to be much faster than on the rest of the surface.[24] The selective growth of LDHs on a microscale in the most active zones is intrinsic to the structure of the AA2024 alloy, but can be carefully controlled by the manipulation of synthesis conditions including the concentration of reactants and pH.

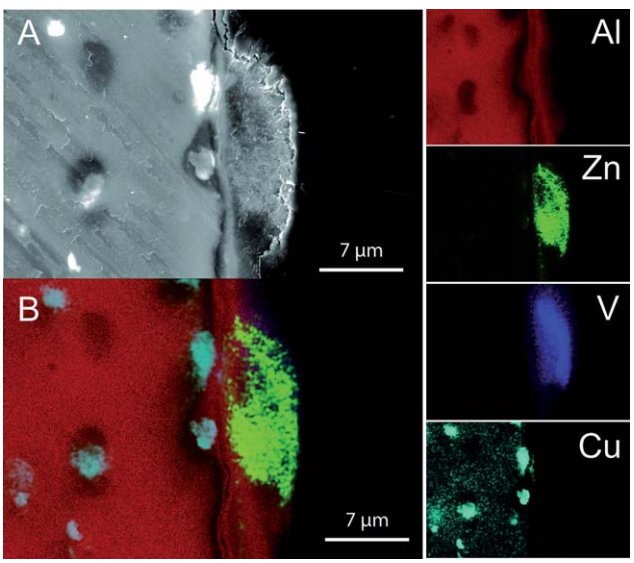

Fig. 2 SEM images (cross-section) of Zn–Al LDH intercalated with $V_2O_7^{2-}$ (A) and its corresponding EDS analysis (B). Individual EDS maps for elements Al, Zn, V and Cu are also presented.

The anticorrosion performance of uncoated and coated AA2024 plates was evaluated after immersion in 0.05 M NaCl solution. Optical photographs (Fig. 3) were acquired at specific immersion times for all the samples. The photographs denote the appearance of AA2024 plates in the beginning (25 minutes) and after 1 month of exposure to a NaCl solution. In the case of bare metal (panels A1 and A2), some small white deposits can already be detected for very short immersion times, indicating the initiation of corrosion processes. After 1 month of immersion, the evidence of corrosion is much more pronounced with the entire surface completely corroded, exhibiting several black pits and compact deposits of white corrosion products over the exposed surface. Contrastingly, the plates coated with LDH films barely show any signs of corrosion. In the case of LDHs intercalated with NO_3^-, only two black pits surrounded by white deposits of corrosion products are observed after 1 month of immersion (B1 and B2), whereas in the case of LDH–V_2O_7 the surface is intact except one minor passivated pit (not presented in the figure), indicating the superior corrosion protection due to ion-exchange driven release of the corrosion inhibitor entrapped in the LDH structure (C1 and C2). Furthermore, sample C was studied before and after immersion in NaCl solution by SEM (Fig. 4). As it can be seen, there is a change neither in terms of individual LDH islands (panels (A) and (B)) nor in the general morphology of the LDH layer (panels (C) and (D)) indicating that the LDH layer is stable under immersion. Besides, the absence of small pits evidences the anticorrosion performance conferred by the protective layer to the underlying aluminium alloy.

The LDH-containing samples were also characterized with XRD in different stages of the immersion to confirm the 'smart' release of the inhibitor from the LDH-container layer in the presence of aggressive chloride ions. The chloride-triggered release was already demonstrated in the case of LDH powders with similar composition.[20] Fig. 1 shows the XRD patterns of the AA2024 samples covered with Zn(2)–Al–V_2O_7 and immersed in 0.05 M NaCl solution for 2 weeks (4) and 1 month (5). The observed shift of the characteristic reflections (003) and (006) indicates a decrease of the basal plane spacing, certainly related to a substitution of $V_2O_7^{2-}$ by Cl^-. As opposed to the anion exchange, $NO_3^- \leftrightarrow V_2O_7^{2-}$,[18] the Zn(2)–Al–$V_2O_7$ and Zn(2)–Al–Cl phases do not coexist during the exchange process. Instead, a new LDH phase appears with a basal spacing value intermediate between the values characteristic of these LDH phases (0.943 and 0.775 nm, respectively).[17,18] These findings suggest some sort of solid solution where pyrovanadate anions are diluted with chlorine anions.

It has been shown[25] that the basal spacing of a layered solid does not depend linearly on a molar ratio of the intercalated ions but exhibits a more complex (non-Vegard's law) behavior. The relationship between the basal spacing d and the composition x (relative amount of the component with a higher d-value) is described by a superlinear function:[25,26]

$$d_n(x) = 1 - (1 - x)^p \quad (1)$$

This journal is © The Royal Society of Chemistry 2011

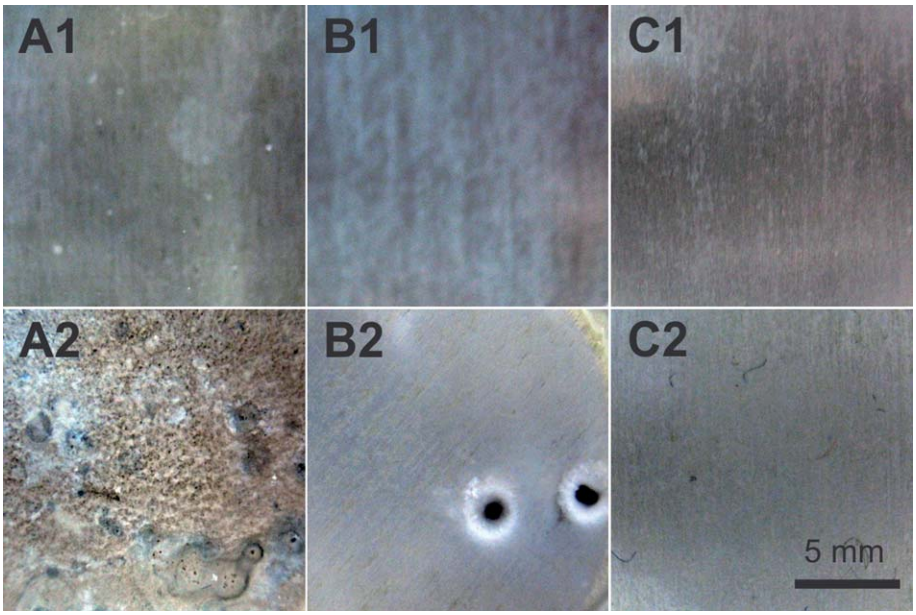

Fig. 3 Photographs acquired for AA2024 plates in the beginning (1) and after 1 month (2) of immersion in 0.05 M NaCl: (A) bare metal, (B) LDH–NO_3 and (C) LDH–V_2O_7.

Published on 05 September 2011 on http://pubs.rsc.org | doi:10.1039/C1JM12463C
Downloaded by Universidade de Aveiro (UAveiro) on 20 July 2012

where d_n is the normalized basal spacing, which is by definition

$$d_n(x) = \frac{d(x) - d(0)}{d(1) - d(0)} \quad (2)$$

and p is the so-called interlayer rigidity parameter.

Using eqn (1) and (2), the values of x corresponding to the observed basal spacings of the (x)Zn(2)–Al–V_2O_7 – $(1 - x)$Zn(2)–Al–Cl LDHs (Fig. 1) were estimated. The parameter p was taken to be 5, as it has previously been determined for a series of the Zn(2)–Al–CO_3 – Zn(2)–Al–Cl LDHs.[26] It was found that after 2 weeks of continuous immersion, approximately half of the $V_2O_7^{2-}$ anions have been substituted by Cl^-, while after 1 month of continuous immersion about 90% of vanadate anions were replaced by chlorides. Thus, even after contact with a NaCl solution for a long period of time, the LDH layer is still capable of storing and delivering on-demand pyrovanadate anions necessary to protect the substrate for subsequent immersion times.

The EIS (Electrochemical Impedance Spectroscopy) spectra corresponding to the samples depicted in Fig. 3 are presented in Fig. 5. The EIS method allows quantitative analysis of the evolution of the corrosion relevant physical parameters during the accelerated immersion tests. For the sake of interpretation, the spectra are divided into three frequency regions according to the time-constants detected: region I (high frequencies, $f > 10^4$ Hz), region II (intermediate frequencies, f-10^0 to 10^1 Hz) and region III (low frequencies f-10^{-2} to 10^{-1} Hz). At the beginning of immersion, the bare AA2024 exhibits one time-constant at intermediate frequencies, assigned to the response of the electrochemical activity at the surface (corrosion processes). The scattering of points at low frequencies is associated with non-stationary conditions due to the active–passive localised corrosion activity. In the case of AA2024 plates covered with LDHs, the magnitude of impedance is considerably higher than for the bare substrate. For the alloy covered with Zn(2)–Al–NO_3 and Zn(2)–Al–V_2O_7, three time constants can be detected: one at high frequencies ascribed to the LDH layer, a second one at intermediate frequencies associated with the response of the native oxide film, and one close to the low frequency end assigned to the corrosion activity.

The impedance values in the frequency region associated with the LDH layer response (region I) are considerably low for LDH–NO_3 films but at least one order of magnitude higher for LDH–V_2O_7. The anion-exchange reaction brings opposing factors into play. In fact, one would expect that the LDH–NO_3 layer demonstrates better barrier properties than the LDH–V_2O_7 one, because of partial defragmentation of the crystallites during the anion exchange (as mentioned above) resulting in some thinning-down of the layer. At the same time, the barrier properties are also dependent upon mobility of the ionic species in the intergallery space of LDH. NO_3^- can move more easily in the LDH galleries than $V_2O_7^{2-}$, the latter being tightly held to the hydroxide layers.[17] This factor could explain the difference in the barrier properties observed in favour of the vanadate-containing LDH structure.

The most relevant results are those observed for long immersion times (1 month, panel (B)). The impedance of bare AA2024 and alloy coated with Zn(2)–Al–NO_3 decreases about one order of magnitude with respect to the initial values. For the bare metal, a steady state condition has been reached with the metal surface fully corroded, and covered with white corrosion products (recall Fig. 3A2). In this case, two time constants are detected, at intermediate and at low frequencies. The former is assigned to the occurrence of corrosion activity, whereas the latter is attributed to processes controlled by mass transport. For the alloy covered with Zn(2)–Al–NO_3, three time constants are observed, two at intermediate frequencies and another one at low frequencies. The assignment of the time constants in the

Published on 05 September 2011 on http://pubs.rsc.org | doi:10.1039/C1JM12463C
Downloaded by Universidade de Aveiro (UAveiro) on 20 July 2012

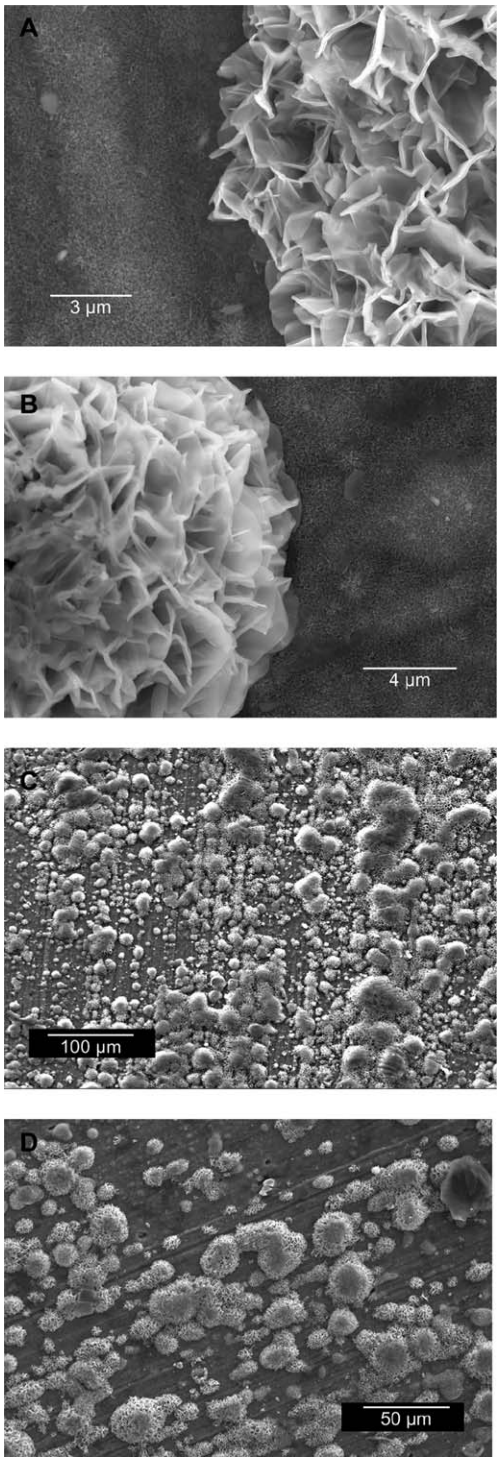

Fig. 4 SEM images of AA2024 plates covered with Zn–Al–V_2O_7 LDHs presented in Fig. 3C before (A and C) and after immersion in 0.05 M NaCl for 1 month (B and D).

intermediate frequency range is not straightforward. From the values obtained from fittings (see the section below) together with visual inspection of the plates, we reached the conclusion that the native aluminium oxide layer response was no longer detected, due to breakage as a result of corrosion attack (recall Fig. 3B2, black pits and corrosion products are detected after 1 month of immersion). Then, the two time constants detected at

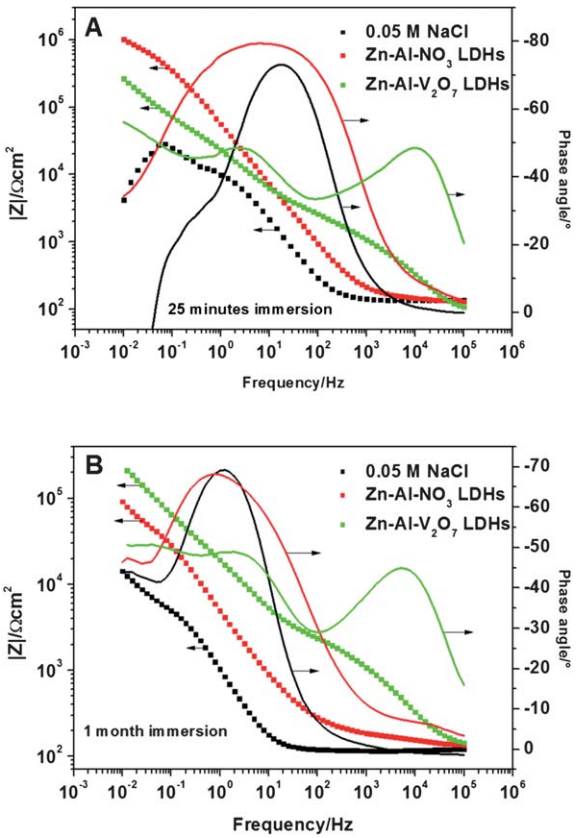

Fig. 5 EIS spectra of AA2024 plates immersed in 0.05 M NaCl for different times.

intermediate frequencies are related to the response of surface deposits (~10 Hz) whilst the time constant at ~1 Hz is ascribed to corrosion activity and double-layer response. The low-frequency time constant is ascribed to processes controlled by mass transport. Contrastingly, the variation of impedance of AA2024 coated with Zn(2)–Al–V_2O_7 is minor, resembling similar to the initial spectra depicted in panel (A). The behaviour observed in the presence of LDH–V_2O_7 can be explained by the active corrosion protection provided by this layer that stores the corrosion inhibitor and gradually releases it in the presence of chloride ions. Moreover, the phase angle for the identified time constants does not surpass 50°. This can be due to diffusion controlled processes ongoing on the coated surface, with the existence of LDH islands in the IMC phases, consequent limitation of oxygen diffusion into the referred sites and hindering of oxygen reduction reaction.

Fig. 6 depicts the evolution of parameters extracted by fitting of EIS spectra using appropriate equivalent circuits. The differences in LDH coating resistance R_{coat} between LDH–NO_3 and LDH–V_2O_7 were already addressed in the qualitative description of the EIS spectra. The graph displayed in Fig. 6A shows that the difference in resistance is more than 1 order of magnitude, with LDH–V_2O_7 showing the highest values. In the case of LDH–NO_3, after 1 hour of immersion the coating response is no longer detectable.

The aluminium oxide present on the alloy surface is the last barrier against aggressive species, and the oxide layer resistance (R_{ox}) gives an indication of the effectiveness of the active

 This journal is © The Royal Society of Chemistry 2011

Published on 05 September 2011 on http://pubs.rsc.org | doi:10.1039/C1JM12463C
Downloaded by Universidade de Aveiro (UAveiro) on 20 July 2012

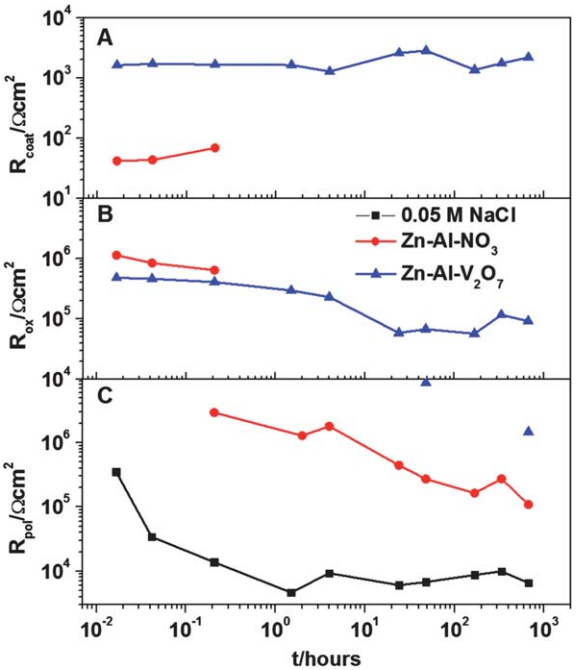

Fig. 6 Evolution of coating resistance (R_{coat}), oxide resistance (R_{ox}) and polarization resistance (R_{pol}) during the immersion time in 0.05 M NaCl. Parameters extracted from fittings of EIS spectra.

protection provided by inhibiting species (Fig. 6B). Initially, the highest R_{ox} was observed in AA2024 covered with LDH–NO_3. This implies that the changes occurring in the native aluminium oxide with the additional step of anion exchange must be considered. In particular, the alkaline pH conditions used to control the desired speciation of vanadates for corrosion purposes (pH = 8–9) may also contribute for the partial dissolution of aluminium oxide in the form of AlO_2^-. This dissolution could be accelerated during the exchange of nitrate with pyrovanadate, when the electrical resistance in the pore gallery is low. In the work of Zhang and colleagues,[13] the LDH structure was grown on top of a thick alumina oxide film purposely obtained by electrochemical techniques where this effect would become 'diluted'. Herein, one makes use of the naturally occurring, *nanometre*-sized, aluminium oxide film as the source of aluminium cations to produce LDHs, on the AA2024 surface. Nonetheless, after 1 hour of immersion, the oxide resistance is no longer detected for the AA2024/LDH–NO_3, which is consistent with the occurrence of localized corrosion. (Open circuit potential measurements performed before the EIS measurement evidences the occurrence of activation/passivation processes.) In the case of LDH–V_2O_7, this parameter decreases at a slower rate than for LDH–NO_3. More importantly, R_{ox} starts to increase again after 1 week of immersion. This increase can be associated with some sort of self-healing of the oxide layer due to the presence of the corrosion inhibitor. Nevertheless, further experiments are required to fully test this effect.

With respect to the polarization resistance associated with the occurrence of corrosion activity, R_{pol}, the results support the superior protection provided by LDH–V_2O_7 (Fig. 6C). The missing points in the graph arise from the impossibility of quantifying the large R_{pol}. After 1 month of immersion, R_{pol} (LDH–V_2O_7) is 1 order of magnitude higher than R_{pol} (LDH–NO_3) and 2 orders of magnitude higher than R_{pol} (bare). The comparison of results for Zn(2)–Al–NO_3 and Zn(2)–Al–V_2O_7 systems emphasizes the importance of the presence of corrosion inhibitors to confer active corrosion protection to the aluminium substrate, especially for long immersion times. Additionally, the high surface area associated with the island-like morphology of these thin LDH structures is certainly an important parameter to favour the adhesion of subsequent coating layers.

3. Experimental

Materials

All the chemicals were obtained from Aldrich, Fluka and Riedel-de Häen, with ≥98% of ground substance, and used as received.

Preparation of aluminium alloys

AA2024 plates were rinsed successively with deionised H_2O, followed by ethanol for removal of particulates and degreasing. Then, the samples were immersed in dilute NaOH solution and HNO_3 to promote alkaline and acid etching, respectively. Each step was followed by washing with deionised H_2O. Finally, the AA2024 plates were sonicated in ethanol for a few minutes and dried in air.

Synthesis of LDH structure

The cleaned AA2024 plates were then immersed in a diluted Zn$(NO_3)_2$ solution with a pH in the neutral range for a few hours under hydrothermal treatment (T < 100 °C). Subsequently, the plates were washed with ultrapure H_2O, ethanol, and dried in air (Zn(2)–Al–NO_3 was obtained). Zn(2)–Al–V_2O_7 was obtained by immersion of Zn(2)–Al–NO_3 coated plates in a $NaVO_3$ solution with a specific basic pH (8–9) for a few hours under hydrothermal treatment (T < 50 °C). The pH control is important to obtain the desired vanadate species in terms of corrosion inhibiting properties.

Examination methods

Phase content and crystal structure of the samples were studied by X-ray diffraction (XRD). Diffraction data were collected at room temperature using a Philips X'Pert MPD diffractometer (Bragg–Brentano geometry, Cu Kα radiation, tube power 40 kV, 50 mA; X'celerator detector, and the exposition corresponded to 11 s per step of 0.02° over the angular range 4 < 2θ < 90°).

Particle morphology and composition were characterized by Scanning Electron Microscopy with Energy Dispersive Spectroscopy (SEM-EDS) (Hitachi S-4100 microscope with an electron beam energy of 25 kV).

EIS measurements were carried out in a three-electrode cell with a saturated calomel reference electrode, a platinum foil counter-electrode and the aluminium alloy sample as the working electrode (exposed area of *ca.* 3 cm^2). The cell was placed in a Faraday cage to avoid the interference of external electromagnetic fields. The electrolyte was 0.05 M NaCl aqueous solution (10 mL). The measurements were performed using a Gamry FAS2 Femtostat with a PCI4 Controller. The selected

frequency range was from 10^5 to 10^{-2} Hz, with a 10 mV of sinusoidal perturbation with 10 points per frequency decade. All the spectra were recorded at open circuit potential. The impedance plots were fitted using different equivalent circuits with the ZView software version 3.1c. The equivalent circuits used were based on RC circuits (instead of pure capacitances, constant phase elements were used), and the goodness of the fittings evaluated by the value of χ^2 (lower than 7×10^{-3}).

4. Conclusions

The methodology hereby presented for the synthesis of LDH-coated AA2024 was shown to allow the formation of a spatially differentiated LDH structure, using the surface active points (located at IMC sites) of the aluminium alloy for this purpose, which are in fact the most important places to be protected from the corrosion standpoint. The resulting nanostructured layer is expected to provide good adhesion. The results demonstrate, for the first time, active corrosion protection by intercalation of corrosion inhibitors ($V_2O_7^{2-}$) in an LDH protective layer. This simple methodology is easy to implement at an industrial level as it does not require exotic conditions, being also environmentally friendly. A new type of self-healing protective coating systems can be developed integrating such LDH-container layers. Moreover, this concept can be easily applied to other fields such as biocide/anti-fouling protection, (bio)chemical sensors, or drug-delivery systems.

Acknowledgements

JT thanks FCT for Post-Doctoral grant (Ref. SFRH/BPD/64335/2009). FCT projects PTDC/CTM/65632/2006 and REDE/1509/RME/2005 are acknowledged as well.

References

1 D. G. Shchukin, M. L. Zheludkevich, K. Yasakau, S. Lamaka, M. G. S. Ferreira and H. Mohwald, *Adv. Mater.*, 2006, **18**, 1672.
2 M. L. Zheludkevich, D. G. Shchukin, K. A. Yasakau, H. Mohwald and M. G. S. Ferreira, *Chem. Mater.*, 2007, **19**, 402.
3 R. G. Buchheit, H. Guan, S. Mahajanam and F. Wong, *Prog. Org. Coat.*, 2003, **47**, 174.
4 J. Tedim, S. K. Poznyak, A. Kuznetsova, D. Raps, T. Hack, M. L. Zheludkevich and M. G. S. Ferreira, *ACS Appl. Mater. Interfaces*, 2010, **2**, 1528.
5 K. D. Ralston, S. Chrisanti, T. L. Young and R. G. Buchheit, *J. Electrochem. Soc.*, 2008, **155**, C350.
6 J.-Y. Uan, J.-K. Lin and Y.-S. Tung, *J. Mater. Chem.*, 2010, **20**, 761.
7 J. Wang, D. Li, X. Yu, X. Jing, M. Zhang and Z. Jiang, *J. Alloys Compd.*, 2010, **494**, 271.
8 X. Guo, S. Xu, L. Zhao, W. Lu, F. Zhang, D. G. Evans and X. Duan, *Langmuir*, 2009, **25**, 9894.
9 (*a*) F. Cavani, F. Trifiro and A. Vaccari, *Catal. Today*, 1991, **11**, 173; (*b*) C. D. Hoyo, *Appl. Clay Sci.*, 2007, **36**, 103.
10 J. K. Lin, C. L. Hsia and J. Y. Uan, *Scr. Mater.*, 2007, **56**, 927.
11 J.-l. Yi, X.-m. Zhang, M.-a. Chen and R. Gu, *Scr. Mater.*, 2008, **59**, 955.
12 H. Chen, F. Zhang, S. Fu and X. Duan, *Adv. Mater.*, 2006, **18**, 3089.
13 F. Zhang, L. Zhao, H. Chen, S. Xu, D. G. Evans and X. Duan, *Angew. Chem., Int. Ed.*, 2008, **47**, 2466.
14 W. Zhang and R. G. Buchheit, *Corrosion*, 2002, **58**, 591.
15 J. Wang, D. Li, Q. Liu, X. Yin, Y. Zhang, X. Jing and M. Zhang, *Electrochim. Acta*, 2010, **55**, 6897.
16 F. Zhang, M. Sun, S. Xu, L. Zhao and B. Zhang, *Chem. Eng. J.*, 2008, **141**, 362.
17 A. N. Salak, J. Tedim, A. I. Kuznetsova, M. L. Zheludkevich and M. G. S. Ferreira, *Chem. Phys. Lett.*, 2010, **495**, 73.
18 C. Barriga, W. Jones, P. Malet, V. Rives and M. A. Ulibarri, *Inorg. Chem.*, 1998, **37**, 1812.
19 S. K. Poznyak, J. Tedim, L. M. Rodrigues, A. N. Salak, M. L. Zheludkevich, L. F. P. Dick and M. G. S. Ferreira, *ACS Appl. Mater. Interfaces*, 2009, **1**, 2353.
20 M. L. Zheludkevich, S. K. Poznyak, L. M. Rodrigues, D. Raps, T. Hack, L. F. Dick, T. Nunes and M. G. S. Ferreira, *Corros. Sci.*, 2010, **52**, 602.
21 M. Zheludkevich, R. Serra, F. Montemor, I. Salvado and M. Ferreira, *Surf. Coat. Technol.*, 2006, **200**, 3084.
22 F. Leroux and J.-P. Besse, *Chem. Mater.*, 2001, **13**, 3507.
23 (*a*) H. Habazaki, K. Shimizu, P. Skeldon, G. E. Thompson, G. C. Wood and X. Zhou, *Trans. Inst. Met. Finish.*, 1997, **75**, 18; (*b*) P. Campestrini, E. P. M. van Westing, H. W. van Rooijen and J. H. W. de Wit, *Corros. Sci.*, 2000, **42**, 1853.
24 K. A. Yasakau, M. L. Zheludkevich, S. V. Lamaka and M. G. S. Ferreira, *J. Phys. Chem. B*, 2006, **110**, 5515.
25 S. Lee, H. Miyazaki, S. D. Mahanti and S. A. Solin, *Phys. Rev. Lett.*, 1989, **62**, 3066.
26 D. R. Hines, S. A. Solin, U. Costantino and M. Nocchetti, *Phys. Rev. B: Condens. Matter*, 2000, **61**, 11348.

Published on 05 September 2011 on http://pubs.rsc.org | doi:10.1039/C1JM12463C
Downloaded by Universidade de Aveiro (UAveiro) on 20 July 2012

 This journal is © The Royal Society of Chemistry 2011